



COBEM
2021 26th International Congress
of Mechanical Engineering



COB-2021-0411

PARTICLE FRAGMENTATION EFFECT ON THE SOLID FUEL COMBUSTION MODELING IN A DROP TUBE FURNACE

Vítor de Souza Lumertz
Fernando Marcelo Pereira
Juliana Gonçalves Pohlmann
Amanda Tavares de Oliveira
Roberto Coelho Andriotti
Paulo Smith Schneider

Federal University of Rio Grande do Sul (UFRGS) / Combustion Laboratory
Sarmento Leite St, 425, 90046-902, Porto Alegre/RS/Brazil

vitordlumertz@gmail.com

fernando.pereira@ufrgs.br

juliana.pohlmann@ufrgs.br

oliveiratamanda@gmail.com

robertocoelho1994@hotmail.com

pss@mecanica.ufrgs.br

Abstract. *The objective of this paper is to study how the particle fragmentation process affects the modeling of solid fuels combustion in a Drop Tube Furnace (DTF). The model is a one-dimensional Lagrangian model that tracks the particle history within the furnace, including the particle heating, devolatilization and char combustion. The simulation considers the particle size distribution (PSD), dividing the sample in different classes, each one with an initial diameter. An optimization procedure is employed to find kinetic parameters of the fuel by comparison with experimental results. Since smaller particles burn faster, the fragmentation process increases the conversion rate. If this process is ignored, the kinetic parameters obtained from an optimization process may not be representative of the fuel. In this paper, the results of the simulations are compared for both cases when the model includes the particle fragmentation process and when it does not. Among other results, the evolution of the PSD, the burnout curve and the new kinetic parameters can be evaluated.*

Keywords: Particle fragmentation, Kinetic parameters, Numerical modeling, Drop tube furnace, Pulverised fuel

1. INTRODUCTION

Solid fuels are the main source for electric power production in the world. In 2020, electricity generation from coal represented more than 30% of the total. Although biomass is not representative in the world matrix, it represents approximately 9% in Brazil. Thus, the study on how each fuel burns is important to predict the behavior of the particles during combustion, as well as to optimize industrial power plants operation. Furthermore, the increasing use of Computational Fluid Dynamics (CFD) simulations renewed the interest in determining kinetic parameters of pulverised fuels.

Typically, the kinetic parameters of pulverised fuels are obtained by fitting the slope of an Arrhenius plot (Moço et al. (2017) and Costa et al. (2015)), but, as conclusions obtained from Großbaier, Smith (1971 and 1982) and others authors referenced in this text, the particle's conversion rate depends on the heating rate, particle size, oxygen disponibility, among others effects. Therefore, the determination of the kinetic parameters using this usual procedure, which involves some simplifications (for example the assumption of a unique representative diameter for the whole sample) may lead to parameters that are strongly dependent on the specific conditions for which they were obtained. A numerical model can avoid this problem by using a more detailed approach, in which the whole combustion history of the fuel particles are calculated and all the physical and chemical phenomena are considered separately. Therefore, the chemical kinetics effect is isolated, which enhances the accuracy of the results and widens its applicability.

Drop Tube Furnaces (DTF) and entrained flow reactors (EFR) are frequently used in studies of solid fuels because they can provide similar combustion conditions of those found in industrial power plants, such as high heating rates and short residence times. Besides that, these furnaces can provide a one-dimensional flow, uniform temperature and the particles are able to burn without other particles' interference. It gives the opportunity to simulate the experiment with good accuracy and with some simplifications, such as a one-dimensional problem.

Ballester and Jiménez (2005) developed a numerical model to predict the kinetic parameters based on the Lagrangian method, which tracks the particle history within the furnace, including the particle heating, devolatilization,

char combustion and oxygen consumption. The particle size distribution (PSD) is considered by dividing the particles of the sample in different classes, each one with an initial diameter. The proposed model was able to reproduce the experimental results made in an EFR, of which the most important is the burnout curve. In 2007, the same authors implemented the fragmentation process in their model and concluded that the calculated burnout curves fitted even better the experimental results. Beyond that, new kinetic parameters were estimated. Since the fragmentation process increases the total surface area of the particles (considering the entire sample), the reaction rates also increase, thus the original kinetic parameters could not represent the experimental results anymore. Only the model with the fragmentation process was able to reproduce the PSD evolution properly, so the new kinetic parameters are more exact than the older ones.

This work used the model proposed by Ballester and Jiménez as basis to estimate the kinetic parameters of a colombian coal and, moreover, to study the effect of particle fragmentation in the PSD evolution and in the burnout curves. The experiments were performed in a DTF.

2. EXPERIMENTAL WORK

The fuel used in this work is a colombian coal, whose main properties, such as proximate analysis and bulk density, are shown in Table 1. According to ASTM D388, this coal is classified as high volatile bituminous.

Table 1. Fuel Characterization.

	Colombian coal
<i>Proximate Analysis (% , dry basis)</i>	
Ash	7.4
Volatile matter	40.3
Fixed carbon	52.3
<i>Physical characteristics</i>	
Bulk density (kg m ⁻³)	1350

The coal's PSD was evaluated using the laser diffractometer Cilas 1190 Particle Size Analyzer and it is shown in Figure 1. The fuel was prepared in the particle size typical of pulverized systems, so that about more than 90% passed 75 µm sieve and the mean diameter is 43.61 µm. Since particle size strongly affects the conversion rates, the use of the PSD instead of a single mean particle size gives more accuracy in methods used for estimating kinetic parameters from experimental measurements. Therefore, in this model, the sample is divided into classes, each one with an initial particle size, which is used as an input of the method.

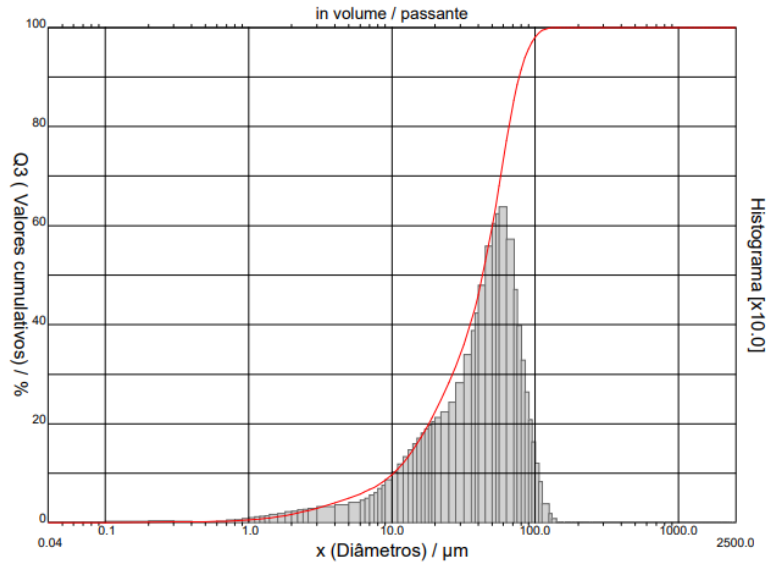


Figure 1. Particle size distribution of the Colombian coal sample.

The combustion tests were performed in a DTF (shown in Figure 2) with a 1.6 m long ceramic tube surrounded by three concentric tubular furnaces, each one with three thermocouples, for control and monitoring furnace temperature. The feeding rate of coal was 55 g/h. The coal was introduced through a water cooled injector placed at the top of the furnace with an air flow rate of 22 L/min. That means that high excess oxygen was a condition of the tests.

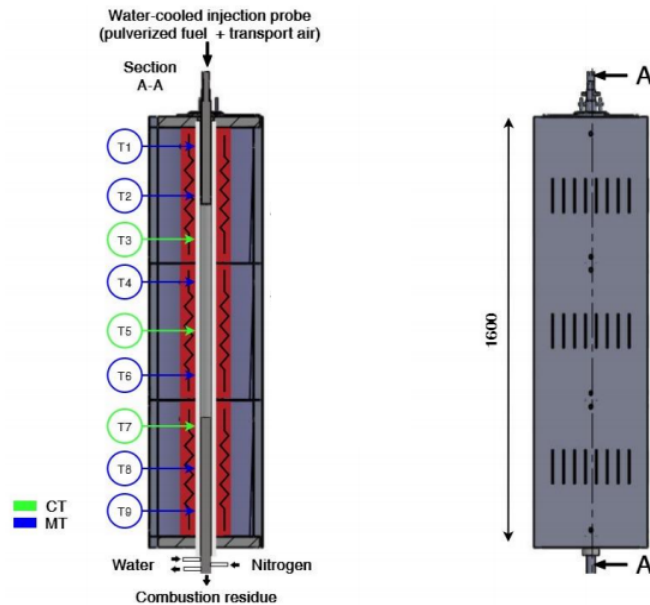


Figure 2. Drop Tube Furnace used in combustion tests. Legend: CT = control thermocouples; MT = monitoring furnace temperature thermocouples.

Samples of partially burned particles were taken in five different points of the furnace (0.3, 0.4, 0.5, 0.6 and 0.7 m of the injector outlet point) and the tests were performed in three different temperatures (1173, 1273 and 1373 K). The samples' PSD and burnout (combustion efficiency) were analyzed and the gas temperature was measured at the same points of the collecting samples with a K-type thermocouple and corrected for radiative and convective heat transfer effects. Each experimental condition, in other words each wall temperature condition, was repeated at least three times to ensure better precision of the measured results. The ash-tracer method, as in Eq. (1), was used to calculate the unburnt fraction, U , which is based on the ash mass fraction in dry basis entering the furnace (Ash_0) and the ash mass fraction in dry basis at the sampling point (Ash).

$$U = \frac{Ash_0 \cdot (1 - Ash)}{Ash \cdot (1 - Ash_0)} \quad (1)$$

The burnout (combustion efficiency) is calculated as $1 - U$.

3. COMBUSTION MODEL

This kinetic parameters determination method is based on simulating the particles' evolution along the DTF, so it is necessary that all phenomena, or at least the main ones, involved in the problem to be modeled. The more the model can reproduce reality and all its physical and chemical phenomena, the more accurate the kinetic parameters obtained are. On the other hand, the parameters are model dependent, which means that if kinetic parameters are used as an input in a CFD code, for example, it should have been estimated with the same combustion model and simplifications.

The model used in this paper is based on: the equation of motion, to determine the velocity and position of the particle in an instant of time; the kinetic equations, to model devolatilization and the fixed carbon (char) burning of along the reactor; the energy balance in the particle, to determine its temperature; the mechanism that describes the variation of the particle's diameter and density; consumption of oxygen to calculate the partial pressure of oxygen along the DTF and finally, the particle fragmentation process. The kinetic parameters are obtained with an optimization process, which varies them until the burnout predicted on a simulation represents the experimental burnout with as little error as possible.

Newton's second law (Eq. 2) is used to predict the particles' velocity, u_p , and position as a function of time. The gravity, buoyant and drag forces are the ones considered in the momentum equation of the particle, which is assumed to be spherical. Stokes regime (laminar flow) was also assumed. The particle momentum equation then reads

$$\frac{\pi}{6} d_p^3 \rho_p \frac{du_p}{dt} = \frac{\pi}{6} d_p^3 g(\rho_p - \rho_g) - 3\pi\mu d_p (u_p - u_g) \quad (2)$$

where d is the diameter, ρ is the density, t is the time, μ is the gas viscosity, g is the gravity acceleration and the subscripts p and g are related to the particle and gas, respectively.

Instantaneous drying was assumed at the injection point and a one-step devolatilization law is used according to

$$\frac{dV}{dt} = -k_V V \quad (3)$$

$$k_V = A_V \cdot \exp\left(\frac{-E_V}{R \cdot T_p}\right) \quad (4)$$

where V is the volatile matter fraction, k is the reaction rate coefficient, A is the pre-exponential factor, E is the activation energy, R is the ideal gas coefficient and T is the temperature. Subscript V is related to the devolatilization process.

The heterogeneous oxidation of char is assumed to happen only at the outer surface area of the particles. It means that their porosity is not considered in this model, since oxygen actually penetrates the particle and combustion can happen inside it as well. The carbon oxidation is modeled as

$$\frac{dC}{dt} = -N \pi d_p^2 k_C \quad (5)$$

with the kinetic parameter and number density given by

$$k_C = A_C P_{O_2,s}^n \exp\left(\frac{-E_C}{R \cdot T_p}\right) \quad (6)$$

$$N = 1/\left((1/6) \pi d_{p,0}^3 \rho_{p,0}\right) \quad (7)$$

where C is the fixed carbon fraction, N is the number of coal per kilogram of coal, $P_{O_2,s}$ is the oxygen partial pressure at the particle's surface and n is the apparent reaction order with respect to O_2 , assumed equal to one.

An energy equation is solved to predict the particle's temperature, which is assumed to be uniform in the whole particle. Radiation, convection, devolatilization and heterogeneous combustion heating rates (Q_R , Q_{conv} , Q_V and Q_C , respectively) are considered in this model. The heat of the volatile matter combustion is assumed to affect the gas temperature more than the particle. Therefore, its heating rate is neglected in the particle's energy equation (Smith 1971). While Q_C is an exothermic heating rate, Q_V is endothermic. Thus, the particle energy equation with the respective source terms are given by

$$\rho_p \frac{1}{6} \pi d_p^3 c_p \frac{dT_p}{dt} = -Q_C + Q_V + Q_{conv} + Q_{rad} \quad (8)$$

$$Q_V = \frac{1}{N} \frac{dV}{dt} H_V \quad (9)$$

$$Q_C = \frac{1}{N} \frac{dC}{dt} H_C \quad (10)$$

$$Q_{conv} = \pi d_p Nu k_g (T_g - T_p) \quad (11)$$

$$Q_{rad} = \pi d_p^2 \varepsilon \sigma (T_w^4 - T_p^4) \quad (12)$$

where c_p is the particle's specific heat, H is the enthalpy, Nu is the Nusselt number, assumed equal to two, k_g is the thermal conductivity of the gas, ε is the particle's emissivity, σ is the Stefan-Boltzmann constant and T_w is the temperature of the furnace's wall.

Particle's density and diameter evolution is modeled as

$$d_p = d_{p,0} (m_p/m_{p,0})^\alpha \quad (13)$$

$$\rho_p = \rho_{p,0} (m_p/m_{p,0})^\beta \quad (14)$$

with α and β respecting the following restriction from mass conservation

$$3\alpha + \beta = 1 \quad (15)$$

where m_p is the particle's mass and the subscript 0 represents the injection point. α and β are parameters that depend on the fuel characteristics. Usually, in CFD codes, α is taken as zero in the devolatilization step; and in the char combustion step, β is assumed as zero. In this work, both parameters are constant and devolatilization and char combustion may happen simultaneously, because of the high heating rate occurring in the tests.

The fragmentation process, the main point of this work, can be modeled by different ways found in the literature, but some complex modeling, for example the models of Senneca (2017) and Liu (2000), depends on fuel's characteristics as particles pores that are difficult to measure. Rabaçal et al. (2018) made observations of single particle fragmentation with a high-speed camera and concluded that three fragmentation modes were detected, affected by the fuel type and the oxidant mixture. Jiménez and Ballester (2007) developed a simple method by creating some fragmentation events, in which a mass fraction of a class, ϕ , is fragmented and each particle becomes two particles with equal size. In this work, the fragments create a new class of particles. ϕ is assumed to be proportional to the unburnt variation, as

$$\phi = \theta \cdot \Delta U \quad (16)$$

where θ is a constant used to predict the experimental PSD.

At the particle surface, oxygen diffusion must balance oxygen consumption by combustion as.

$$2\pi N d_p D_{O_2} \frac{M_{O_2}}{RT_p} (P_{O_{2,g}} - P_{O_{2,s}}) = \frac{1}{v_{c,CO}} \pi N d_p^2 A_c P_{O_{2,s}}^n \exp\left(\frac{-E_c}{RT_p}\right) \quad (17)$$

where D_{O_2} and M_{O_2} are the mass diffusivity and the molecular mass of oxygen, respectively; $P_{O_{2,g}}$ is the oxygen partial pressure of the gas far away from the particles and $v_{c,CO}$, equal to 0.75, is the mass-based stoichiometric ratio of heterogeneous oxidation considering that CO is the only product of the particle's combustion. After that, the CO gas is also oxidized, thus CO_2 is finally produced. Sherwood number is assumed equal to 2, as in Hayhurst (2000).

The partial pressure of oxygen of the gas, $P_{O_{2,g}}$, is estimated according to the mass of char and volatile matter consumed, as shown below.

$$\frac{M_{O_2} G}{\rho_g RT_g} (P_{O_{2,g,0}} - P_{O_{2,g}}) = \frac{1}{v_v} (V_0 - \sum_j w_j V_j) + \frac{1}{v_{c,CO_2}} (C_0 - \sum_j w_j C_j) \quad (18)$$

where G is the ratio between the mass flow of gas and fuel at the beginning of the DTF, w is the mass fraction of each class j and v_v is the mass-based stoichiometric ratio of devolatilization, equal to 0.25. Notice that in Eq.18 the mass-based stoichiometric ratio of heterogeneous oxidation is equal to 0.375, because of the CO oxidation, as discussed earlier. In Eq 18, Methane is assumed to be the only volatile matter.

4. RESULTS

PSD and burnout of the samples collected in the different points of the DTF were measured. Figure 3 shows the PSD of the original coal (blue line) and the PSD of the char at three different points of the reactor when wall temperature was set to 900°C. Actually, PSD measurements were made in 1000°C and 1100°C as well, but the authors think that the experimental results of the lowest temperature (900°C) are more consistent, so, for brevity, most of the results shown in this work is for this wall temperature.

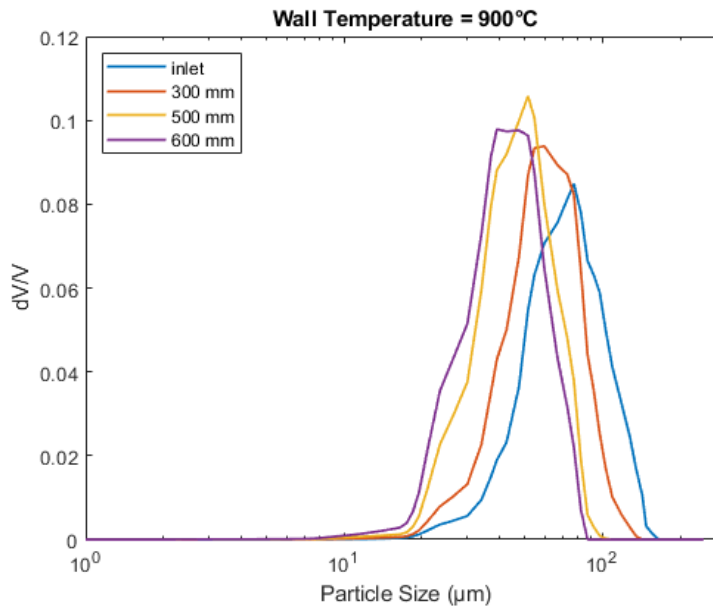


Figure 3. PSD measurements of the colombian coal at the injector point (blue line) ,and the PSD of the char at three different points of the reactor when wall temperature was setted to 900°C. The Y-axis represents the fraction of volume of a certain class of particle.

The PSD profiles shown in Fig. 3 are very similar to those presented in Jiménez and Ballester paper (2007). The diameter D_{43} was plotted against the burnout considering the ashes $(1 - m/m_0)$ in Figure 4 and compared with the curves of Eq. (13) for different alphas.

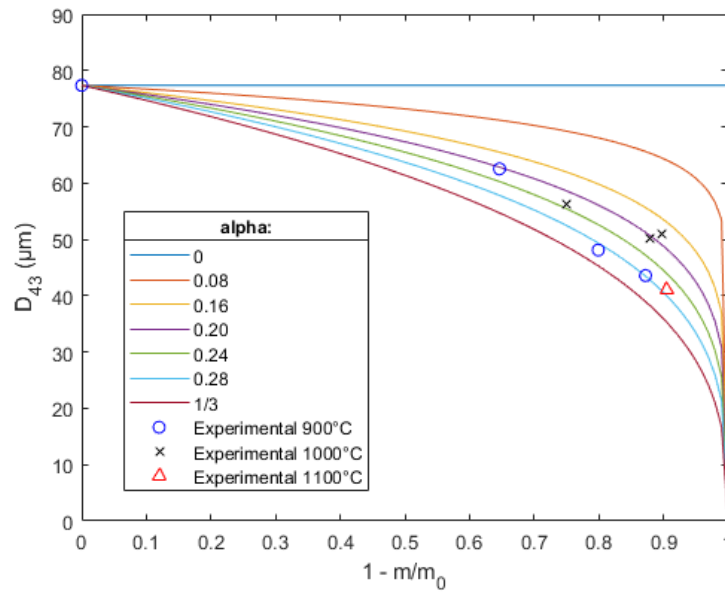


Figure 4. Measurements of $D_{43}(1-m/m_0)$ in comparison to Eq. (13) with different alphas.

Alpha is set equals to 0.24 in the simulations because of the better fit to the experimental data. The decrease of the D_{43} with an intermediate alpha (between zero and $1/3$, which are the minimum and maximum values respectively) indicates that diameter and density vary at the same time, typical of regime II of combustion (Smith 1971).

To study the fragmentation effects on the burnout curves and in the PSD evolution, it is necessary to simulate the problem without this phenomenon for comparison. Table 2 presents the optimized parameters for this both cases (with and without fragmentation) and the deviation between the experimental and calculated burnout points. The optimization process adjusted the experimental burnout data with the calculated curve without fragmentation first. Then, in a second moment, the A_c passed through the same process to adjust the burnout curve with the new model, considering particle fragmentation. Therefore, the kinetic parameters, except for the A_c , are the same for all simulations. Figure 5 shows the burnout curves with and without the fragmentation effect. The best value for θ is 1.2, value used in all the simulations with particle fragmentation in this work. Jiménez and Ballester (2007) used this parameter equal to 1.7, for comparison.

Table 2. Optimized Parameters.

	Without Fragmentation	With Fragmentation
A_c ($\text{kg m}^{-2} \text{s}^{-1} \text{Pa}^{-1}$)	1.65×10^{-4}	1.48×10^{-4} (-10.3%)
E_c (kJ/mol)	44.0	=
A_v (s^{-1})	3.04×10^{-6}	=
E_v (kJ/mol)	65.5	=
Deviation (%)	1.66	=

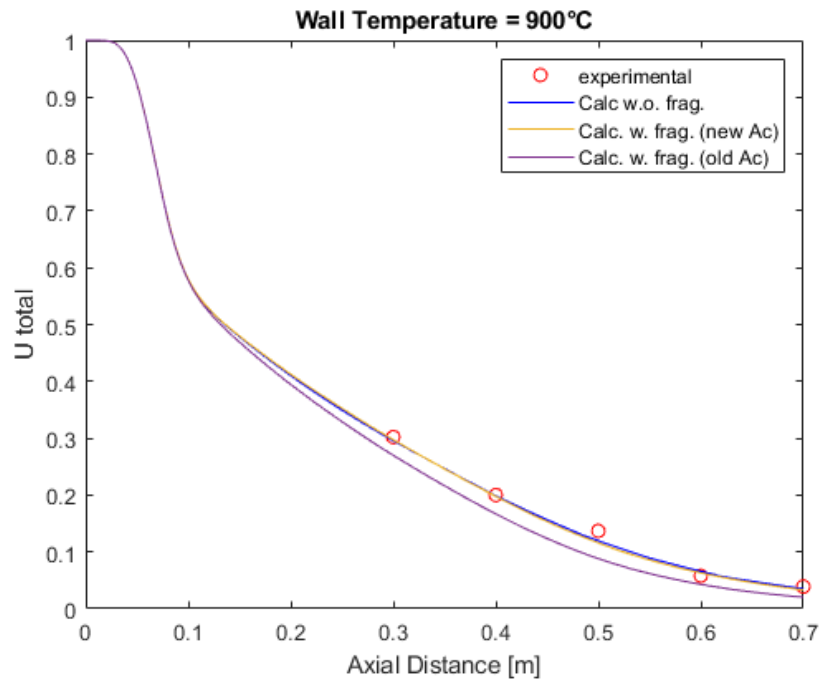


Figure 5. Burnout curves with and without fragmentation.

It is visible the difference when we change the model without changing the parameters. As expected, the combustion rate is bigger with particle fragmentation; and thus it is needed to calculate the new A_c , which corresponds, in this case, to a reduction of 10.3% of the original one (calculated without fragmentation). This reduction was bigger for the experiments of Jiménez and Ballester (2007): 28,6%. In this paper, the burnout curves considering and not considering the fragmentation process are practically the same, but Jiménez and Ballester could get a better curve with the new model, which made the deviation decrease.

Although it is possible to predict the experimental burnouts without modeling the fragmentation process, the calculated PSD only had results similar to reality when particle fragmentation was taken into account. The evolution of D43 considering and desconsidering fragmentation is shown in Figure 6, as well as the Eq. (13) curve with alpha is equal to 0.24. Each step in the yellow line (with fragmentation) is one fragmentation event of a certain class. These events occur in a time interval of 0.2s. Smaller intervals than 0.2s does not affect the final result very much.

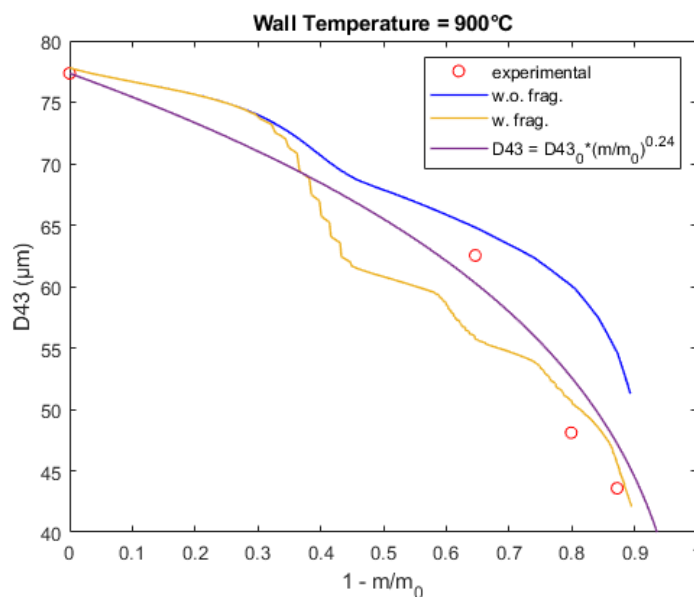


Figure 6. Evolution of D43 with and without fragmentation and in comparison with the experimental data.

Notice that the blue D43 curve (without fragmentation) is not similar to the purple one (Eq. (13)), since it has all the particle classes influence. Differently from the burnout curves, Figure 6 shows a better fit curve with the fragmentation effect. Simulations with alpha equal to 1/3 were also made and even though it is the biggest alpha allowed in the model (the most diameter variation possible), it was not able to predict the two last points as the simulation with fragmentation did (with alpha equal to 0.24).

Figure 7 compares the PSD evolution on different points of the DTF between experimental data and simulations with and without the fragmentation model. The Y-axis (dV/V) represents the volume fraction contained in a diameter range. The dash-dot lines are in the maximum values of the experimental curves and help us to compare with the other two graphs, which were calculated from the simulations.

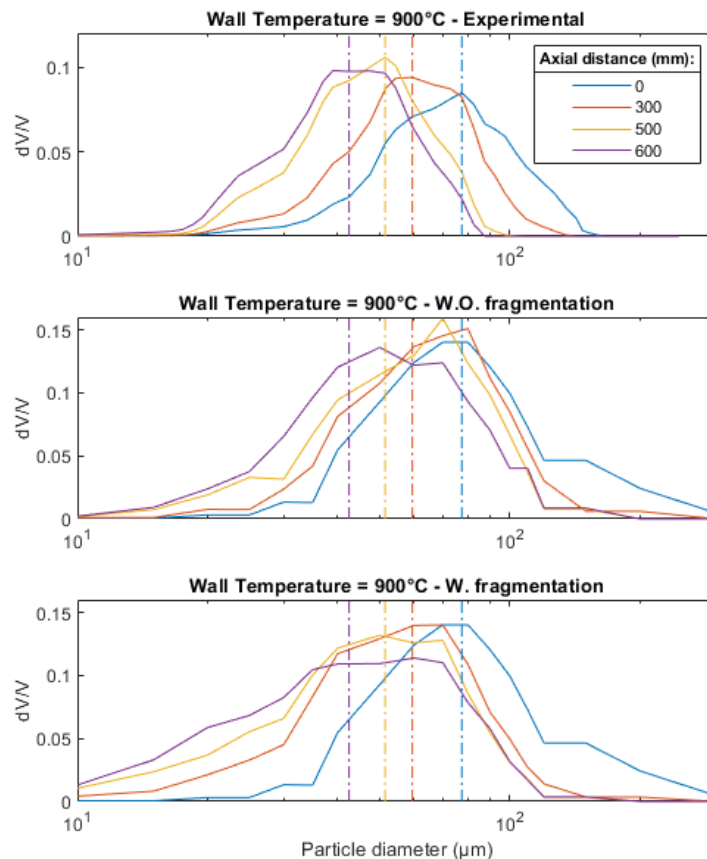


Figure 7. PSD evolution. Comparison between experimental and simulated data.

The curves are not smooth because it was necessary to make a move mean in the graphs to eliminate the noise produced by the characteristic of discrete particles in different classes. However, these graphs can still be used to compare the general format and the maximum values. Notice that when the fragmentation is not taken into account (second graph), the maximum points of the inlet, 300 and 500 mm are very close to each other, differentially from what happens in the experimental curves and also with the last graph curves, when fragmentation is considered. Figure 7 also remarks on the production of thin particles, in the range of 20 - 30 μm , caused by the fragmentation process.

5. CONCLUSION

Fragmentation is a process that changes particle size distribution and, consequently, affects the reaction rates of experiments. If this process is taken into account, it makes the simulations more accurate, and the chemical kinetics can be isolated from other phenomena with more precision. Therefore the optimized kinetic parameters obtained when particle fragmentation is considered are more representative for the fuel under analysis if compared with those obtained without taking it into account. Keeping all parameters constant except for A_c , the fragmentation model made A_c decrease 10.3% in the optimization process.

PSD and burnout curves obtained in experiments can be better reproduced if fragmentation is considered. Actually, in this work, the calculated burnout curves are practically the same with and without fragmentation, with 1.66% of

deviation from the experimental burnout points. The more the physical and chemical phenomena are well reproduced by mathematical models, the more independent the kinetic parameters are from the specific experimental conditions. This work was able to implement one more phenomenon in a solid fuels combustion model and to get results that were observed experimentally. The PSD curves presented a somewhat improved behavior with fragmentation. However, additional experimental results are necessary for optimizing the model parameters.

6. ACKNOWLEDGEMENTS

This work was supported by Coordenação de Aperfeiçoamento de Pessoal de Nível Superior - Capes, by Conselho Nacional de Desenvolvimento Científico e Tecnológico – CNPq and by Fundação de Amparo à Pesquisa do Estado do Rio Grande do Sul (FAPERGS). The authors also gratefully acknowledge Porto do Pecém Geração de Energia S.A. for providing the colombian coal sample.

7. REFERENCES

- Ballester, J. and Jiménez, S., 2005. “Kinetic parameters for the oxidation of pulverized coal as measured from drop tube tests”. *Combustion and Flame*, Vol. 142, pp. 210–222.
- Costa, A. et al., 2015. “Combustion kinetics and particle fragmentation of raw and torrefied pine shells and olive stones in a drop tube furnace”. *Proceedings of the Combustion Institute*, Vol. 35, pp. 3591–3599.
- Großbaier, C. “Single coal particle combustion”. *ET-B1 Clean Fossil Fuels*.
- Hayhurst, A.N., 2000 “The Mass Transfer Coefficient for Oxygen Reacting with a Carbon Particle in a Fluidized or Packed Bed”. *Combustion and Flame*, Vol. 121, pp. 679-688.
- Jiménez, S. and Ballester, J., 2007. “Study of the evolution of particle size distribution and its effects on the oxidation of pulverized coal”. *Combustion and Flame*, Vol. 151, pp. 482–494.
- Liu, G. et al., 2017 “Modeling the fragmentation of non-uniform porous char particles during pulverized coal combustion”. *Fuel*, Vol. 79 pp. 627–633.
- Moço, A. et al., 2017 “Combustion Behavior of Coals From Thermogravimetric and Drop Tube Furnace Experiments”. *MCS 10 - Naples, Italy, September 17-21, 2017*.
- Pohlmann, J.G., Lumertz, V.S., Andriotti, R.C. Mortari, D.A., Brune, M.C., Hayashi, T.C., Schneider, P.S. and Pereira, F.M., 2020. “Validation of a one-dimensional numerical model to predict solid fuel combustion in a drop tube furnace”. In *Proceeding of the 18th Brazilian Congress of Thermal Sciences and Engineering – ENCIT 2020*. Porto Alegre, Brazil.
- Rabaçal, M. et al., 2018. “Direct observations of single particle fragmentation in the early stages of combustion under dry and wet conventional and oxy-fuel conditions”. *Proceedings of the Combustion Institute*, Vol. 000, pp. 1–8.
- Senneca, O. et al., 2017 “Prediction of structure evolution and fragmentation phenomena during combustion of coal: Effects of heating rate”. *Fuel Processing Technology*, Vol. 166 pp. 228–236.
- Smith, I.W., 1971. “Kinetics of Combustion of Size Graded Pulverized Fuels in the Temperature Range 1200-2270 K”. *Combustion and Flame*, Vol. 17, pp. 303-314.
- Smith, I.W., 1971. “The Kinetics of Combustion of Pulverized Semi-Anthracite in the Temperature Range 1400-2200 K”. *Combustion and Flame*, Vol. 17, pp. 421-428.
- Smith IW., 1982. “The combustion rates of coal chars: a review”. *Nineteenth Symposium (International) on Combustion/The Combustion Institute*, pp. 1045-1065.

8. RESPONSIBILITY NOTICE

The authors are the only responsible for the printed material included in this paper.